EPJ Web of Conferences **175**, 13007 (2018) https://doi.org/10.1051/epjconf/201817513007
Lattice 2017

D meson semileptonic form factors in $N_f = 3$ QCD with Möbius domain-wall quarks

Takashi Kaneko[1,2,⋆], *Brian* Colquhoun[1], *Hidenori* Fukaya[3], and *Shoji* Hashimoto[1,2]
(JLQCD Collaboration)

[1] *High Energy Accelerator Research Organization (KEK), Ibaraki 305-0801, Japan*
[2] *SOKENDAI (The Graduate University for Advanced Studies), Ibaraki 305-0801, Japan*
[3] *Osaka University, Osaka 560-0043, Japan*

Abstract. We present our calculation of $D \to \pi$ and $D \to K$ semileptonic form factors in $N_f = 2 + 1$ lattice QCD. We simulate three lattice cutoffs $a^{-1} \simeq 2.5$, 3.6 and 4.5 GeV with pion masses as low as 230 MeV. The Möbius domain-wall action is employed for both light and charm quarks. We present our results for the vector and scalar form factors and discuss their dependence on the lattice spacing, light quark masses and momentum transfer.

1 Introduction

The $D \to K\ell\nu$ and $\pi\ell\nu$ semileptonic decays provide a precise determination of the Cabibbo-Kabayashi-Maskawa (CKM) matrix elements $|V_{cs}|$ and $|V_{cd}|$, respectively. The hadronic matrix element for the $D \to P\ell\nu$ decay ($P = \pi, K$) is described by the vector and scalar form factors $f^{DP}_{\{+,0\}}$ as

$$\langle P(p')|V_\mu|D(p)\rangle = \left(p + p' - \frac{M_D^2 - M_P^2}{q^2} q\right)_\mu f_+^{DP}(q^2) + \frac{M_D^2 - M_P^2}{q^2} q_\mu f_0^{DP}(q^2), \tag{1}$$

where $q^2 = (p - p')^2$ is the momentum transfer. Due to parity symmetry of QCD, the semileptonic and leptonic decays are sensitive to interactions with different Dirac structures: in the Standard Model, for instance, only the weak vector (axial) current contributes to the semileptonic (leptonic) decays. These two decay processes are therefore complementary probes of new physics. In contrast to the leptonic decays, the hadronic uncertainty of the form factors limits the accuracy of the determination of $|V_{cs(d)}|$ and new physics search, due to less precise lattice QCD calculations and more precise experimental data [1]. The JLQCD Collaboration launched an independent calculation of the D meson semileptonic form factors on fine lattices [2, 3]. This article updates the status of this project.

2 Simulation method

We simulate $N_f = 2 + 1$ QCD using the tree-level improved Symanzik gauge action and the Möbius domain wall quark action [4]. Our choice of the sign function approximation and the kernel operator in

⋆ Speaker, e-mail: takashi.kaneko@kek.jp

its four-dimensional effective action largely reduces the computational cost compared to our previous works with the overlap fermion, and it enables us to simulate large lattice cutoffs $a^{-1} \gtrsim 2.5$ GeV [5] with good chiral symmetry. At $a^{-1} \sim 2.5$ and 3.6 GeV, we take three values of degenerate up and down quark mass, m_{ud}, and two values of strange quark mass m_s close to its physical value $m_{s,\mathrm{phys}}$. The range of the pion mass is 300 MeV $\lesssim M_\pi \lesssim$ 500 MeV. For a better control of the continuum and chiral extrapolations, we extend these simulations to a finer lattice at $a^{-1} \sim 4.5$ GeV with $M_\pi \sim 300$ MeV, as well as to a lighter pion mass $M_\pi \sim 230$ MeV at $a^{-1} \sim 2.5$ GeV. Depending on a^{-1} and m_{ud}, we employ a spatial lattice size L satisfying a condition $M_\pi L \gtrsim 4$ in order to control finite volume effects. The statistics are 5,000 Molecular Dynamics time at each simulation point. Simulation parameters are summarized in Table 1. The main progress since the previous report [3] is that we have completed two simulations at our largest a^{-1} and smallest M_π.

At the large cutoffs 2.5 – 4.5 GeV, we can also safely employ the same domain-wall action for charm quarks. The charm quark mass is fixed to the physical value determined from the low-lying charmonium spectrum. The renormalized mass in the $\overline{\mathrm{MS}}$ scheme $m_c(3\ \mathrm{GeV}) = 1.003(10)\,\mathrm{GeV}$ [6] is consistent with the present world average. We also note that chiral symmetry is preserved to good accuracy at these cutoffs. The residual quark mass is $O(1\ \mathrm{MeV})$ at $a^{-1} \sim 2.5$ GeV and even smaller ($\lesssim 0.2$ MeV) at finer lattices with moderate sizes in the fifth dimension ~ 10.

We extract the $D \to P$ matrix element (1) from the three-point function

$$C^{DP}_{V_\mu}(\mathbf{p}, \mathbf{p}'; \Delta x_4, \Delta x'_4) = \frac{1}{N_s^3\, N_{x_{4,\mathrm{src}}}} \sum_{x_{4,\mathrm{src}}} \sum_{\mathbf{x},\mathbf{x}',\mathbf{x}''} \langle O_P(\mathbf{x}', x_{4,\mathrm{src}} + \Delta x_4 + \Delta x'_4) \times V_\mu(\mathbf{x}'', x_{4,\mathrm{src}} + \Delta x_4) O^\dagger_D(\mathbf{x}, x_{4,\mathrm{src}}) \rangle e^{-i\mathbf{p}'(\mathbf{x}'-\mathbf{x}'')} e^{-i\mathbf{p}(\mathbf{x}''-\mathbf{x})}, \quad (2)$$

where $N_s = L/a$, and $O_{\{D,P\}}$ represents the meson interpolating field with a Gaussian smearing. The initial D meson is at rest ($\mathbf{p} = 0$), and we simulate four values of the momentum transfer q^2 by taking the final light meson momenta with $|\mathbf{p}'|^2 = 0, 1, 2, 3$ in units of $(2\pi/L)^2$.

In our measurement of $C^{DP}_{V_\mu}(\mathbf{p}, \mathbf{p}'; \Delta x_4, \Delta x'_4)$, we fix the total temporal separation $\Delta x_4 + \Delta x'_4$ and vary the location of the vector current Δx_4. We choose $\Delta x_4 + \Delta x'_4 = 28a$ at $a^{-1} \sim 2.5$ GeV by inspecting the stability of the form factor results against $\Delta x_4 + \Delta x'_4$ [2]. The physical length of $\Delta x_4 + \Delta x'_4$ is the

Table 1. Simulation parameters. Quark masses are bare value in lattice units. The rightmost column shows the number of temporal locations of the meson source operator of correlation functions.

lattice parameters	m_{ud}	m_s	M_π[MeV]	M_K[MeV]	$N_{x_{4,\mathrm{src}}}$
$\beta = 4.17$, $a^{-1} = 2.453(4)$, $32^3 \times 64 \times 12$	0.0190	0.0400	499(1)	618(1)	2
	0.0120	0.0400	399(1)	577(1)	2
	0.0070	0.0400	309(1)	547(1)	4
	0.0035	0.0400	226(1)	525(1)	4
	0.0190	0.0300	498(1)	563(1)	2
	0.0120	0.0300	397(1)	518(1)	2
	0.0070	0.0300	310(1)	486(1)	4
$\beta = 4.35$, $a^{-1} = 3.610(9)$, $48^3 \times 96 \times 8$	0.0120	0.0250	501(2)	620(2)	2
	0.0080	0.0250	408(2)	582(2)	2
	0.0042	0.0250	300(1)	547(2)	4
	0.0120	0.0180	499(1)	557(2)	2
	0.0080	0.0180	408(2)	516(2)	2
	0.0042	0.0180	296(2)	474(2)	4
$\beta = 4.47$, $a^{-1} = 4.496(9)$, $64^3 \times 128 \times 8$	0.0030	0.0150	284(1)	486(1)	4

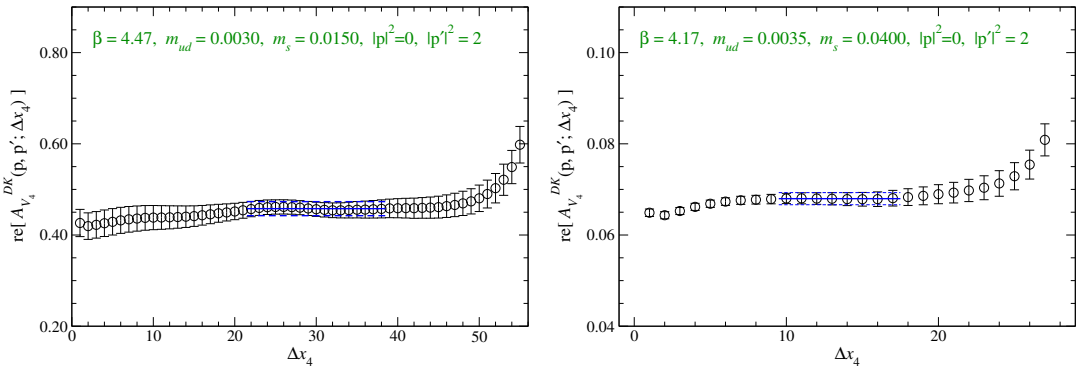

Figure 1. Effective value of amplitude $A^{DK}_{V_4}(\mathbf{p},\mathbf{p}')$ for $D\to K$ decay as a function of Δx_4. The left panel shows data at the largest cutoff $a^{-1}\sim 4.5$ GeV ($\beta=4.47$ and $M_\pi\simeq 300$ MeV), whereas the right panel is for the smallest $M_\pi\simeq 230$ MeV ($\beta=4.17$, $a^{-1}\sim 2.5$ GeV). The D meson is at rest, and the squared magnitude of the kaon momentum is $|\mathbf{p}'|^2=2$ in units of $(2\pi/L)^2$.

same for the other two cutoffs. In order to improve the statistical accuracy, $C^{DP}_{V_\mu}$ is averaged over the location of the meson source operator $(\mathbf{x}, x_{4,\mathrm{src}})$ as indicated in Eq. (2). We employ the volume source generated with Z_2 noise to average over $\mathbf{x}$ at a given time-slice $x_{4,\mathrm{src}}$. This measurement is repeated over $N_{x_{4,\mathrm{src}}}$ different values of $x_{4,\mathrm{src}}$. Table 1 shows our choice of $N_{x_{4,\mathrm{src}}}$. The correlation of $C^{DP}_{V_\mu}$ among different $x_{4,\mathrm{src}}$'s is not large with the small values of $N_{x_{4,\mathrm{src}}}=2-4$. We observe about a factor of $\sqrt{N_{x_{4,\mathrm{src}}}}$ improvement in the statistical accuracy.

We also calculate two-point functions of π, K and D mesons

$$C^Q(\mathbf{p};\Delta x_4) \;=\; \frac{1}{N_s^3\,N_{x_{4,\mathrm{src}}}}\sum_{x_{4,\mathrm{src}}}\sum_{\mathbf{x},\mathbf{x}'}\langle O_Q(\mathbf{x}',x_{4,\mathrm{src}}+\Delta x_4)O_Q^\dagger(\mathbf{x},x_{4,\mathrm{src}})\rangle e^{-i\mathbf{p}(\mathbf{x}'-\mathbf{x})}\quad (Q=\pi,K,D) \tag{3}$$

in a similar way. The amplitudes of these correlation functions are extracted from the following fit in terms of Δx_4

$$C^{DP}_{V_\mu}(\mathbf{p},\mathbf{p}';\Delta x_4,\Delta x_4') \;=\; A^{DP}_{V_\mu}(\mathbf{p},\mathbf{p}')e^{-E_D(\mathbf{p})\Delta x_4}e^{-E_P(\mathbf{p}')\Delta x_4'}\qquad (P=\pi,K), \tag{4}$$

$$C^Q(\mathbf{p};\Delta x_4) \;=\; B^Q(\mathbf{p})e^{-E_Q(\mathbf{p})\Delta x_4}\qquad (Q=\pi,K,D), \tag{5}$$

where we estimate the meson energies $E_{\{\pi,K,D\}}$ from their rest masses and the dispersion relation in the continuum limit. Figure 1 shows examples of the effective value of $A^{DP}_{V_\mu}(\mathbf{p},\mathbf{p}')$. We observe reasonably long plateaus and can also reliably determine the amplitudes at the largest a^{-1} and smallest M_π.

We evaluate the $D\to P$ matrix element as

$$\langle P(\mathbf{p}')|V_\mu|D(\mathbf{p})\rangle \;=\; 2Z_V\sqrt{\frac{E_D(\mathbf{p})\,E_P(\mathbf{p}')\,|A^{DP}_{V_\mu}(\mathbf{p},\mathbf{p}')|^2}{B^D(\mathbf{p})\,B^P(\mathbf{p}')}}, \tag{6}$$

where we employ the renormalization factor Z_V calculated non-perturbatively in Ref. [7]. The relevant semileptonic form factors are then extracted via Eq. (1).

3 Parameter dependence of form factors

Figure 2 compares results for $f^{D\pi}_{\{+,0\}}$ among different values of a^{-1} (left panel) and M_π (right panel). We observe reasonably good consistency among the lattice data and also with the experimental data

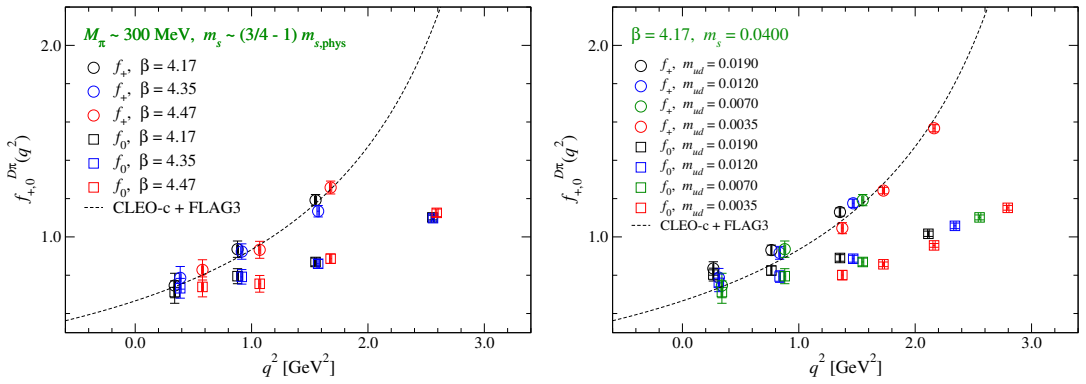

Figure 2. Left panel: comparison of $D \to \pi$ form factors among different values of a^{-1}. We plot data of $f_+^{D\pi}(q^2)$ (circles) and $f_0^{D\pi}(q^2)$ (squares) at $M_\pi \sim 300$ MeV and at the larger m_s as a function of q^2. Right panel: comparison of $D \to \pi$ form factors among different values of M_π. We plot data at $\beta = 4.17$ and $m_s = 0.0400$. In both panels, the dashed line shows the Becirevic-Kaidalov parametrization [10] of the CLEO-c data for $f_+^{D\pi}$ [8] with the normalization $f_+^{D\pi}(0)$ fixed to the world average by the Flavor Lattice Averaging Group (FLAG) [11].

of $f_+^{D\pi}$ [8]. This suggests that $f_{\{+,0\}}^{D\pi}$ mildly depends on a^{-1} and M_π from our simulation region down to $a = 0$ and the physical pion mass $M_{\pi,\mathrm{phys}}$. We note that our choice of the lattice action and cutoffs also leads to small discretization errors for the decay constant $f_{D_{(s)}}$ [9].

Similar to our observation in the previous report [3], the momentum transfer dependence of $f_{\{+,0\}}^{DP}(q^2)$ is well described by the model independent expansion in terms of a small parameter [12]

$$z(t, t_0) = \frac{\sqrt{t_+ - q^2} - \sqrt{t_+ - t_0}}{\sqrt{t_+ - q^2} + \sqrt{t_+ - t_0}} \tag{7}$$

also at the largest a^{-1} and smallest M_π. Here $t_+ = (M_D + M_P)^2$ is the DP threshold energy. The free parameter t_0 is set to an optimized value $t_0 = (M_D + M_P)(\sqrt{M_D} - \sqrt{M_P})^2$, such that the magnitude $|z|$ is small in the semileptonic region. In this article, we employ the so-called Bourrely-Caprini-Lellouch (BCL) parametrization [13]

$$f_{\{+,0\}}^{DP}(q^2) = \frac{1}{B_{\{+,0\}}(q^2)} \sum_{k=0}^{N_{\{+,0\}}} a_{\{+,0\},k}\, z^k \tag{8}$$

to determine the normalization $f_+^{DP}(0) = f_0^{DP}(0)$.

For $f_+^{DK(\pi)}$, we use the vector meson mass $M_{D_s^*}$ (M_{D^*}) measured at each simulation point as the resonance mass in the Blaschke factor $B_+(q^2) = 1 - q^2/M_{D_s^*(D^*)}^2$. The z dependence of f_+^{DP} is well approximated by the pole factor $1/B_+(q^2)$, and $N_+ = 1$ already gives reasonable $\chi^2/\mathrm{d.o.f.} \lesssim 1$. Since we have not yet calculated the scalar meson masses, $M_{D_{s0}^*}$ nor $M_{D_0^*}$, it is not clear whether there exist isolated poles below the threshold t_+ at the simulated values of M_π. We employ a simple linear fit in z by setting $N_0 = 1$ and $B_0(q^2) = 1$, which also yields $\chi^2/\mathrm{d.o.f.} \lesssim 1$. The systematic uncertainty due to the choice of the parametrization form is estimated by testing the quadratic function ($N_+ = 2$) for f_+^{DP}, and the Blaschke factor $B_0(q^2) = 1 - q^2/M_{D_{s0}^*(D_0^*)}^2$ for f_0^{DP} with the experimental values of $M_{D_{s0}^*}$ and $M_{D_0^*}$. The systematic error turns out to be comparable or smaller than the statistical uncertainty.

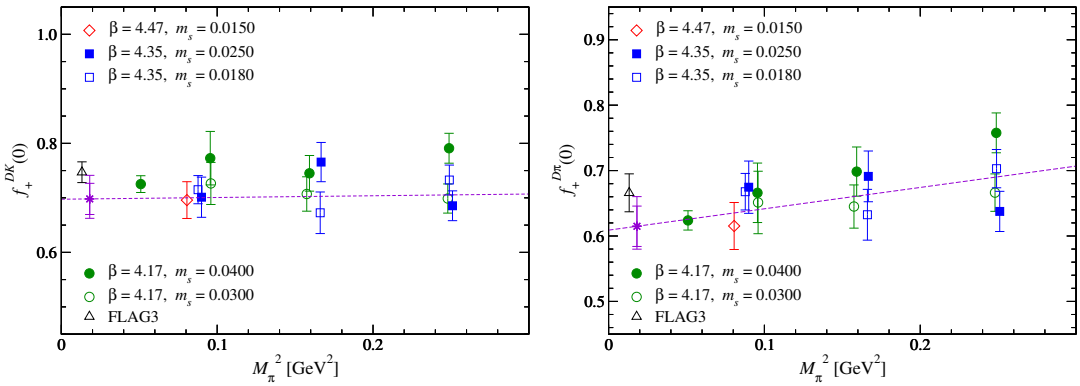

Figure 3. Continuum and chiral extrapolation for $f_+^{DK}(0)$ (left panel) and $f_+^{D\pi}(0)$ (right panel). We plot $f_+^{DK(\pi)}$ at different a and m_s by different symbols as a function of M_π^2. The dashed line represent the fit line (9) at $a=0$ and the physical strange quark mass $m_{s,\mathrm{phys}}$. We also plot the recent FLAG average [11] by the open triangle.

Having observed the mild dependence on the lattice spacing and quark masses in Fig. 2, we extrapolate $f_+^{DP}(0)$ to the physical point in the continuum limit by using a simple linear extrapolation

$$f_+^{DP}(0) = c^{DP} + c_a^{DP} a^2 + c_\pi^{DP} M_\pi^2 + c_{\eta_s}^{DP} M_{\eta_s}^2, \tag{9}$$

where $M_{\eta_s}^2 = 2M_K^2 - M_\pi^2 \propto m_s$. Figure 3 shows this continuum and chiral extrapolation for f_+^{DK} and $f_+^{D\pi}$. As expected from Fig. 2, we obtain good values of $\chi^2/\mathrm{d.o.f} \sim 1.0-1.3$, and most coefficients (except $c_\pi^{D\pi}$) are consistent with zero. We estimate the systematic uncertainty by including a quadratic term for the M_π^2 dependence of $f_+^{D\pi}(0)$ and by removing each linear term for other parameter dependences. Our numerical results are

$$f_+^{DK}(0) = 0.698(29)_{\mathrm{stat}}(-18)_{q^2\to 0}\binom{+32}{-12}_{a\to 0,\mathrm{chiral}}, \tag{10}$$

$$f_+^{D\pi}(0) = 0.615(31)_{\mathrm{stat}}\binom{+17}{-16}_{q^2\to 0}\binom{+28}{-7}_{a\to 0,\mathrm{chiral}}, \tag{11}$$

where the first error is statistical error, and the second (third) error is the systematic uncertainty due to the q^2 (continuum and chiral) extrapolation. As seen in Fig. 3, our results are consistent with the recent FLAG averages [11].

We obtain $|V_{cs}| = 1.035(^{+64}_{-53})_{\mathrm{lat}}(5)_{\mathrm{exp}}$ and $|V_{cd}| = 0.232(^{+17}_{-13})_{\mathrm{lat}}(3)_{\mathrm{exp}}$ by using recent experimental input $|V_{cs(d)}|\, f_+^{DK(\pi)}(0)$ compiled by the Heavy Flavor Averaging Group (HFAG) [14]. This estimate satisfies CKM unitarity in the second row $|V_{cd}|^2 + |V_{cs}|^2 + |V_{cb}|^2 = 1.13(0.14)$, where $|V_{cb}|$ has small effects, and hence the tension between the exclusive and inclusive decays does not distort unitarity. It is well known that the uncertainty of $f_+^{DK(\pi)}(q^2_{\mathrm{ref}})$ at a reference q^2_{ref} increases toward the conventional reference point $q^2_{\mathrm{ref}} = 0$ [1]. As in recent lattice studies of B meson semileptonic decays, it is better to make comparison between lattice QCD and experiments in a wide region of q^2.

4 Global fit of form factors

In this article, we carry out a global fit of the form factors as a function of a, M_π^2 and $M_{\eta_s}^2$ based on SU(2) hard pion heavy meson chiral perturbation theory (hard pion HMChPT) [16], while the pionic

[1] This is a good reference point for $K\to\pi\ell\nu$, since $SU(3)$ flavor breaking effects are quadratic in small symmetry-breaking parameter $m_s - m_u$ [15].

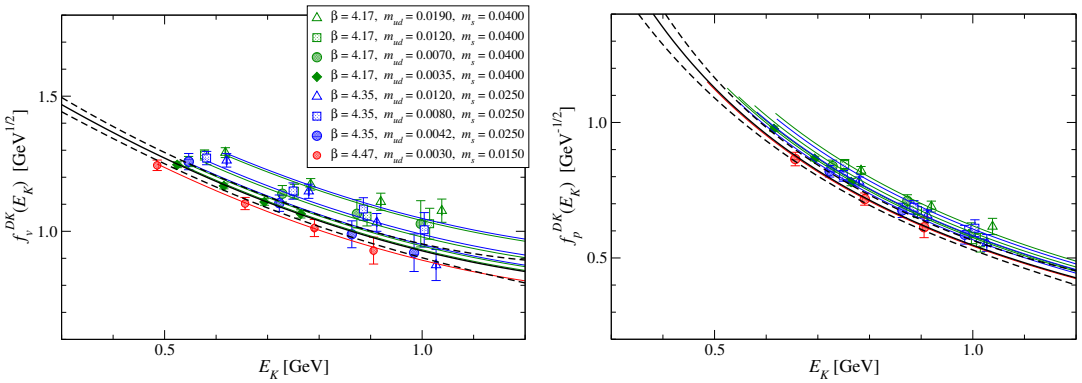

Figure 4. Global fit for f_v^{DK} (left panel) and f_p^{DK} (right panel). For clarity, we plot $f_{\{v,p\}}^{DK}$ only at larger m_s as a function of E_K, while the global fit is carried out by using all data. Different symbols show data at different a and M_π. The thick lines show the fit curve at $M_{\pi,\mathrm{phys}}$ and at $a=0$.

logarithms have been calculated in both heavy meson and relativistic formulations. To this end, we use the form factors in the following decomposition convenient for the heavy meson formulation

$$\langle P(p')|V_\mu|D(p)\rangle \;=\; \sqrt{M_D}\left\{v_\mu\, f_v^{DP}(E_P) + (p' - E_P v)_\mu\; f_p^{DP}(E_P)\right\}, \tag{12}$$

where $v = p/M_D$ is the D meson 4-velocity, and $E_P = vp'$ is the light meson energy in the D rest frame. We note that $1/m_Q$ dependence of $f_{\{v,p\}}^{D\pi}$ turns out to be mild even at $m_Q = m_c$ in our study of the $B\to\pi\ell\nu$ decay [17]. We leave a global fit based on the relativistic parametrization (1) and that in conventional HMChPT [18, 19] for our future analysis to study the systematic uncertainty.

We employ a parametrization form

$$f_v^{DP}(E_P) \;=\; c_v^{DP}\left\{f_{\log}^{DP} + c_{v,\pi}^{DP} M_\pi^2 + c_{v,\eta_s}^{DP} M_{\eta_s}^2 + c_{v,E}^{DP} E_P + d_{v,E}^{DP} E_P^2 + c_{v,a}^{DP} a^2\right\}, \tag{13}$$

$$f_p^{DP}(E_P) \;=\; \frac{c_p^{DP}}{E_P + \Delta M_D}\left\{f_{\log}^{DP} + c_{p,\pi}^{DP} M_\pi^2 + c_{p,\eta_s}^{DP} M_{\eta_s}^2 + c_{p,E}^{DP} E_P + d_{p,E}^{DP} E_P^2 + c_{p,a}^{DP} a^2\right\} \tag{14}$$

from our observation in the previous subsection. Namely, we include the linear terms to describe the mild dependence on a, M_π^2 and $M_{\eta_s}^2$, whereas a quadratic term is added for the dependence on E_P, which is related to q^2 through $E_P = (M_D^2 + M_P^2 - q^2)/2M_D$. We include the pole factor with $\Delta M_D = M_{D_{(s)}^*} - M_D$ for f_p^{DP}, which is proportional to the matrix elements with the spatial vector current $\langle P|V_k|D\rangle$. The chiral logarithm is given as $f_{\log}^{DP} = (c_{\log}^{DP}/\Lambda_\chi^2)\log\left[M_\pi^2/\Lambda_\chi^2\right]$ with $\Lambda_\chi = 4\pi f$, $c_{\log}^{D\pi} = -3(1+3g^2)/4$ and $c_{\log}^{DK} = 1/2$. We fix the decay constant in the chiral limit f to the FLAG average [11] and the $D^*D\pi$ coupling to $g = 0.61$ [20].

As shown in Fig. 4, the parametrizations (13) and (14) describe our data well and yield $\chi^2/\mathrm{d.o.f} \sim 0.9$ ($f_{\{v,p\}}^{DK}$) and 1.2 ($f_{\{v,p\}}^{D\pi}$). The coefficients for the a, M_π^2 and $M_{\eta_s}^2$ dependences are not large. We emphasize that $c_{\{v,p\},a}^{DP}$ is consistent with zero, which suggests small discretization error for $f_{\{v,p\}}^{DP}$.

The global fit for $f_{\{v,p\}}^{DP}$ can be translated into that for $f_{\{+,0\}}^{DP}$ by using the kinematical relation

$$f_+^{DP}(q^2) \;=\; \frac{1}{\sqrt{2M_D}}\left\{f_v^{DP}(E_P) + (M_D - E_P)\; f_p^{DP}(E_P)\right\}, \tag{15}$$

$$f_0^{DP}(q^2) \;=\; \frac{\sqrt{2M_D}}{M_D^2 - M_P^2}\left\{(M_D - E_P)\, f_v^{DP}(E_P) + \left(E_P^2 - M_P^2\right) f_p^{DP}(E_P)\right\}. \tag{16}$$

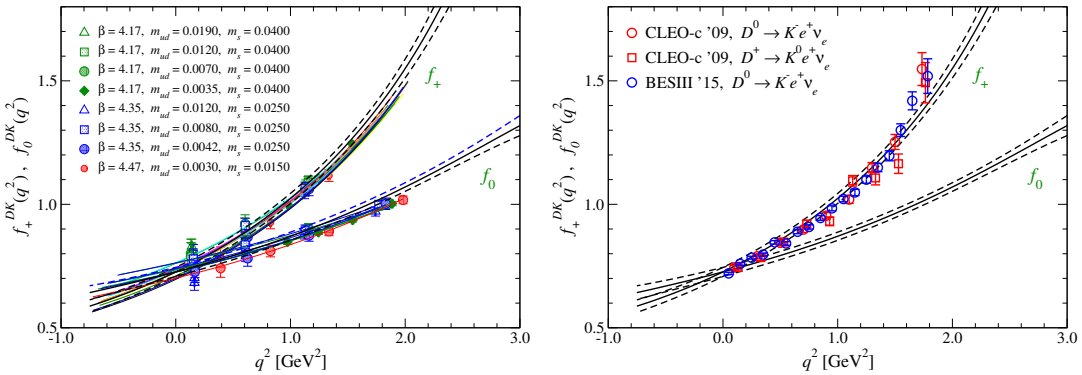

Figure 5. Left panel: global fit for $f^{DK}_{\{+,0\}}$ reproduced from that for $f^{DK}_{\{v,p\}}$. For better visibility, we plot data at larger m_s as a function of q^2. The green, blue and red symbols show data at $a^{-1} \sim 2.5$, 3.6 and 4.5 GeV, respectively, whereas the different symbols show data at different M_π values. The thick lines show the fit curve at the physical point and $a = 0$. We also plot the fit curves at simulation points by thin lines, which are however indistinguishable at the scale of this figure due to the mild a and M_π dependence of $f^{DP}_{\{+,0\}}$. Right panel: comparison of form factor shape between lattice (thick solid lines) and experimental (circles and squares) data.

The left panel of Fig. 5 shows the global fit for $f^{DK}_{\{+,0\}}$, which reproduces the data at simulation points reasonably well.

From experimental data of the partial decay rate $\Delta\Gamma_i$ together with the CKM matrix element $|V_{cs(d)}|$, we can estimate the vector form factor ${f_+}^{DK(\pi)}$ as

$$ {f_+}^{DK(\pi)}(q_i^2) \;=\; \frac{1}{|V_{cs(d)}|}\sqrt{\frac{24\pi^3}{G_F^2}\frac{1}{p_i^3}\frac{\Delta\Gamma_i}{\Delta q_i^2}}, \tag{17} $$

where G_F is the Fermi constant, Δq_i^2 is the size of the i-th q^2 bin, and p_i is the light meson momentum in the D rest frame for the i-th bin. Note that experimental data are available for the light lepton modes $D \to P\{e,\mu\}\nu$, and hence have low sensitively to f_0^{DP}, which is suppressed by the lepton mass squared m_l^2. We estimate f_+^{DP} from the CLEO-c [8] and BESIII [21] data of $\Delta\Gamma_i$ and the HFAG values of the CKM matrix elements [14]. The right panel of Fig. 5 confirms good agreement in the form factor shape between our lattice data and experimental data. This also suggests that we obtain the CKM matrix elements close to their HFAG values when we determine them as a relative normalization factor between the lattice and experimental data.

5 Conclusions

In this article, we update the status of our study of the D meson semileptonic decays. Form factors are calculated on fine lattices with cutoffs up to 4.5 GeV by using the Möbius domain-wall action for both light and charm quarks. We observe good consistency of the normalization ${f_+}^{DK(\pi)}(0)$ with previous lattice calculations and the form factor shape is nicely consistent with experiment.

Having observed small discretization errors at m_c, it is important to extend our simulations to the B meson decays. At this conference, we have reported our studies of the $B \to \pi\ell\nu$ [17] and inclusive [22] decays. Another interesting future direction is an extension to form factors to quantify new physics contributions. Our analysis of the D meson tensor form factors are underway.

Acknowledgment

Numerical simulations are performed on the IBM System Blue Gene Solution at KEK under its Large Scale Simulation Program (No. 16/17-14) and on the Oakforest-PACS supercomputer operated by the Joint Center for Advanced High Performance Computing (JCAHPC). This research is supported in part by JSPS KAKENHI Grant Number JP26247043 and JP26400259, and by MEXT as "Priority Issue on post-K computer" (Elucidation of the Fundamental Laws and Evolution of the Universe) and the Joint Institute for Computational Fundamental Science.

References

[1] T. Kaneko, X.R. Lyu, A. Oyanguren, PoS **CKM2016**, 014 (2017), 1705.05975
[2] T. Suzuki, Y.G. Cho, H. Fukaya, S. Hashimoto, T. Kaneko, J. Noaki, PoS **LATTICE2015**, 337 (2016)
[3] T. Kaneko, B. Fahy, H. Fukaya, S. Hashimoto (JLQCD), PoS **LATTICE2016**, 297 (2017), 1701.00942
[4] R.C. Brower, H. Neff, K. Orginos, Comput. Phys. Commun. **220**, 1 (2017), 1206.5214
[5] T. Kaneko, S. Aoki, G. Cossu, H. Fukaya, S. Hashimoto, J. Noaki (JLQCD), PoS **LATTICE2013**, 125 (2014), 1311.6941
[6] K. Nakayama, B. Fahy, S. Hashimoto, Phys. Rev. **D94**, 054507 (2016), 1606.01002
[7] M. Tomii, G. Cossu, B. Fahy, H. Fukaya, S. Hashimoto, T. Kaneko, J. Noaki (JLQCD), Phys. Rev. **D94**, 054504 (2016), 1604.08702
[8] D. Besson et al. (CLEO), Phys. Rev. **D80**, 032005 (2009), 0906.2983
[9] B. Fahy, G. Cossu, S. Hashimoto, PoS **LATTICE2016**, 118 (2016), 1702.02303
[10] D. Becirevic, A.B. Kaidalov, Phys. Lett. **B478**, 417 (2000), hep-ph/9904490
[11] S. Aoki et al., Eur. Phys. J. **C77**, 112 (2017), 1607.00299
[12] C. Bourrely, B. Machet, E. de Rafael, Nucl. Phys. **B189**, 157 (1981)
[13] C. Bourrely, I. Caprini, L. Lellouch, Phys. Rev. **D79**, 013008 (2009), [Erratum: Phys. Rev.D82,099902(2010)], 0807.2722
[14] Y. Amhis et al. (2016), 1612.07233
[15] M. Ademollo, R. Gatto, Phys. Rev. Lett. **13**, 264 (1964)
[16] J. Bijnens, I. Jemos, Nucl. Phys. **B846**, 145 (2011), 1011.6531
[17] B. Colquhoun, S. Hashimoto, T. Kaneko (JLQCD Collaboration), *$B \to \pi\ell\nu$ with Möbius Domain Wall Fermions*, in *Proceedings, 35th International Symposium on Lattice Field Theory (Lattice2017): Granada, Spain*, to appear in EPJ Web Conf., 1710.07094
[18] A.F. Falk, B. Grinstein, Nucl. Phys. **B416**, 771 (1994), hep-ph/9306310
[19] D. Becirevic, S. Prelovsek, J. Zupan, Phys. Rev. **D68**, 074003 (2003), hep-lat/0305001
[20] V. Lubicz, L. Riggio, G. Salerno, S. Simula, C. Tarantino (ETM), Phys. Rev. **D96**, 054514 (2017), 1706.03017
[21] M. Ablikim et al. (BESIII), Phys. Rev. **D92**, 072012 (2015), 1508.07560
[22] S. Hashimoto, B. Colquhoun, T. Izubuchi, T. Kaneko, H. Ohki (JLQCD Collaboration), *Inclusive B decay calculaitons with analytic continuation*, in *Proceedings, 35th International Symposium on Lattice Field Theory (Lattice2017): Granada, Spain*, to appear in EPJ Web Conf.